Laser-Linewidth-Tolerant Feed-Forward Carrier Phase Estimator With Reduced Complexity for QAM

Jianqiang Li, *Member, IEEE*, Lei Li, Zhenning Tao, *Senior Member, IEEE*, Takeshi Hoshida, *Member, IEEE*, and Jens C. Rasmussen, *Member, IEEE*

***Abstract*—An improved feed-forward carrier phase estimation scheme with further complexity reduction is presented and numerically verified for quadrature amplitude modulation (QAM) formats. Based on the blind phase search (BPS) algorithm, a general two-stage configuration is first derived by removing several restrictions assumed in the prior art. Two guidelines for determining the design parameters are then proposed to minimize the computational complexity while mitigating the pattern effect and maintaining the tolerance to laser linewidth. Taking square 64QAM as an example, the computational efforts can be reduced by a factor of 4 while keeping the same tolerance to laser linewidth as compared to a single-stage BPS estimator.**

***Index Terms*—Carrier phase estimation, coherent detection, feed-forward, optical communications, quadrature amplitude modulation (QAM).**

I. Introduction

THE growing bandwidth demand has imposed great challenges on optical transport networks. Therefore, many efforts have been made on high-capacity and high-speed optical transmission systems [1]. Among diverse enabling techniques, the use of quadrature amplitude modulation (QAM) fueled by coherent detection is an attractive solution [2]–[5]. On one hand, the use of spectrally-efficient QAM formats allows enhancing the channel date rate at no cost of increased optoelectronic bandwidth. On the other hand, the success of employing advanced modulation formats relies on the coherent detection since it enables to access to the full information of optical fields, while resorting to the powerful digital signal processing (DSP) techniques [6], [7].

In contemporary optical coherent systems, the laser phase noise is commonly compensated for by digital carrier phase estimation, which allows the use of free-running local- oscillator (LO) lasers at the receiver side. In practice, the digital carrier phase estimation is desired to be implemented in a blind and feed-forward manner for efficient purpose. Therefore, a number of blind feed-forward carrier phase estimation algorithms have been proposed for quadrature phase-shift keying (QPSK) and square 16 QAM formats [8]–[12]. However, it is intractable to extent these algorithms for higher-order QAM formats due to the stronger susceptibility to laser phase noise and the denser constellations of such formats.

Recently, T. Pfau *et al.* introduced the blind-phase-search (BPS) algorithm (also called the minimum distance method) that was originally proposed for more general synchronous communication systems in [13] and [14] to optical coherent systems [15]. The developed estimator is based on a single-stage configuration. This single-stage BPS estimator features good tolerance to laser linewidth, blind feed-forward manner, and universality to arbitrary QAM formats. Nevertheless, a practical problem associated with the single-stage configuration is its hardware implementation complexity. Several two-stage feedforward carrier phase estimation schemes have been reported to cut down the complexity [16]–[19]. With these schemes, the computational effort has been reduced by a factor ranging from 1.5 to 3 depending on the order of QAM formats. In two of these literatures [16] and [17], the BPS algorithm is employed in only one of the two stages. The BPS-based stage serves as a fine carrier phase estimator in [16], while the BPS-based stage is designed to provide a coarse estimate of the carrier phase in [17]. In contrast to the above two works, both stages utilize the BPS algorithm for the coarse and fine estimations respectively in [18], [19]. Herein, an estimator using BPS algorithm in both stages is referred to as a two-stage BPS estimator in this paper. In [18] and [19], the overall complexity is not significantly reduced since the total number of test-phase angles was not minimized for a two-stage configuration. A critical problem hindering the minimization of test-phase angle number is the pattern effect which has not been analyzed previously. Furthermore, in [18] and [19], the restriction of equal summing window length of two stages also prevents flexible tradeoff between the mitigation of pattern effect and laser linewidth tolerance.

In this paper, an improved two-stage BPS estimation scheme is proposed with further complexity reduction. By removing the restrictions assumed in [18] and [19], the pattern effect is mitigated and the total number of test phase angles of the two stages is minimized while keeping the same tolerance to laser phase noise as the single-stage BPS estimator described in [15].

The rest of the paper is organized as follows. Section II begins with a brief review of the conventional BPS algorithm specified in [15], and then provides an explanation on the pattern effect. Section III first describes the configuration of a general two-

Manuscript received April 19, 2011; revised June 01, 2011; accepted June 06, 2011. Date of publication June 16, 2011; date of current version July 22, 2011.

J. Li was with the Communication Technology Laboratory, Fujitsu R&D Center, 100025 Beijing, China. He is now with the Photonics Laboratory, Department of Microtechnology and Nanoscience, Chalmers University of Technology, Gothenburg, Sweden (e-mail: jqjqlee@gmail.com).

L. Li, and Z. Tao are with the Communication Technology Laboratory, Fujitsu R&D Center, 100025 Beijing, China.

T. Hoshida and J. C. Rasmussen are with Network Systems Laboratories, Fujitsu Laboratories LTD, 211-8588 Kawasaki, Japan.

Color versions of one or more of the figures in this paper are available online at http://ieeexplore.ieee.org.

Digital Object Identifier 10.1109/JLT.2011.2159580

stage BPS estimator derived based on [18] and [19], and then elaborates on the guidelines to minimize the complexity for a two-stage BPS estimator. In Section IV, simulation results are presented. Finally, further discussion and conclusion are made in Sections V and VI.

II. BPS Algorithm and Pattern Effect

A. Conventional BPS Algorithm

Assuming ideal signal detection, clock recovery, equalization, and laser frequency offset compensation, the input symbol-rate sample $r(k)$ to a carrier phase estimator in a typical digital optical coherent receiver can be modeled as

$$r(k) = s(k)e^{j\theta(k)} + n(k) \tag{1}$$

where $s(k)$ denotes the kth transmitted symbol drawn from a QAM constellation; $n(k)$ stands for additive complex white Gaussian noise; and $\theta(k)$ represents the phase noise.

In order to estimate $\theta(k)$, a distance metric $M(\varphi, k)$ is first defined as follows [13]–[15]:

$$M(\varphi,k) = \sum_{n=k-\text{ceil}(N/2)+1}^{k+\text{floor}(N/2)} \left| r(n)e^{j\varphi} - \text{Decision}[r(n)e^{j\varphi}] \right|^2 \tag{2}$$

where Decision $[\cdot]$ denotes hard decision in accordance with the given QAM constellation; φ represents the test phase in the range $[-\pi/4, \pi/4)$ due to the $\pi/2$ rotational symmetry of QAM constellations; floor$(\cdot)$ denotes flooring function; ceil$(\cdot)$ denotes ceiling function; N is an integer and denotes the length of summing window within which the squared Euclidean distances of the symbols are summed up to smooth the additive noise. It can be seen from (2) that the observed sample $r(k)$ is located roughly in the center of the summing window depending on the parity of N. With the defined distance metric, the rule of the BPS algorithm is to find a phase angle having the minimum distance metric, which can be formulated as

$$\hat{\theta}(k) = \text{unwrap}\left[\underset{\varphi\in[-\pi/4,\pi/4)}{\arg\min} M(\varphi,k) \right] \tag{3}$$

where $\hat{\theta}(k)$ denotes the phase estimate for the kth symbol, $\arg\min(A)$ denotes to find a phase φ which makes A minimum, and unwrap$[\cdot]$ stands for the conventional unwrapping operation to overcome cycle slipping.

In practice, it is impossible to solve the above minimization problem over a continuous phase range $[-\pi/4, \pi/4)$. It has been suggested to discretize the test phase φ into a finite set of equidistant phase angles given by

$$\varphi_i = \frac{i\pi}{2I} - \frac{\pi}{4}, \quad i = 0, 1, \ldots, I-1 \tag{4}$$

where i is the index of these discrete phase angles, and I denotes the total number of these phase angles and defines the test-phase resolution. It is worthy to note that I is directly associated with the entire complexity of the estimator since each phase angle requires one time of distance metric computation which consumes considerable efforts according to (2). Hence, one effective way to cut down the ultimate complexity lies in the reduction of the number of test phase angles (i.e., the number of distance-metric computations).

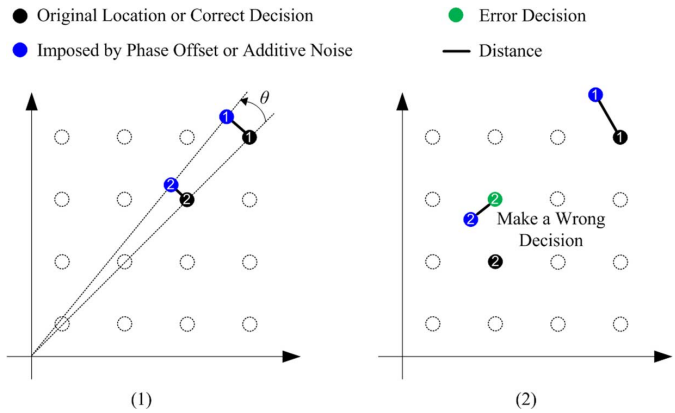

Fig. 1. Two typical cases that contribute to the pattern effect.

B. Pattern Effect

Let us consider (1) and (2). As is known, a symbol $s(k)$ selected from a given QAM constellation may exhibit different discrete amplitudes and have different count of adjacent points around it in the constellation. For the symbols with different amplitudes and different locations in the constellation, even the same amount of additive complex noise $n(k)$ and phase offset $\theta(k)$ may convert to different magnitude of deviation from the hard-decided constellation points. Therefore, the distance metric $M(\varphi, k)$ defined by (2) varies depending on different symbol sequence pattern in an observed summing window. In this paper, this phenomenon is referred to as the pattern effect. Two typical cases that facilitate understanding of the above statement are illustrated in Fig. 1, where the first quadrant of a 64QAM constellation is considered. As for the first case, it can be seen that the same phase offset may lead to different distances for symbols with different amplitudes. Regarding the second case, error decision is more likely to occur for the inner points due to more surrounding points. In this case, the same amount of additive complex noise may likewise lead to different distances.

In principle, the summing window should be sufficiently long so that the impact of the pattern effect is negligible. However, in an optical coherent receiver, the presence of time-varying phase noise induced by laser linewidth and fiber nonlinearity prevents too long summing window for carrier phase estimation. With a limited N, the pattern effect gets more serious in particular for higher-order QAM formats. In order to illustrate this effect, simulations were carried out for square 64QAM with no laser linewidth and a typical signal-to-noise ratio (SNR) per symbol (E_s/N_0) of 23 dB. Fig. 2(a) plots the average distance metric $M(\varphi, k)/N$ as a function of test phase φ with enough resolution (i.e., $I = 256$). Besides the black solid line for a large

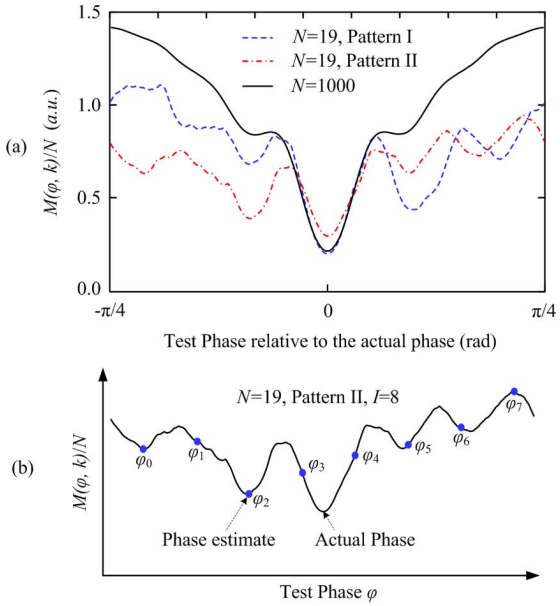

Fig. 2. Illustration of the pattern effect: (a) average distance metric as a function of the test phase and (b) pattern effect results in significant estimation errors for a limited I.

$N = 1000$, there are two examples corresponding to two special symbol patterns for a limited $N = 19$. It can be clearly seen that multiple sharp local minimums appear for these patterns. Fig. 2(b) shows one example in which the pattern effect results in significant estimation error. As can be seen from Fig. 2(b), if the number of test-phase angles I is limited (e.g., $I = 8$), the estimator may detect a phase angle far from the target. The deviation may exceed one minimum search interval. Therefore, the pattern effect should be in particular paid attention to.

III. Complexity-Reduced Two-Stage BPS Estimator

A. General Two-Stage BPS Configuration

In [18] and [19], the overall complexity is not significantly reduced since the total number of test-phase angles was not minimized for a two-stage configuration. In addition, the summing window length is also restricted to be equal for the two stages. Here, it is preferable to derive a more general two-stage BPS estimator by removing the restrictions assumed in [18] and [19]. The block diagram of a general two-stage BPS estimator is shown in Fig. 3. It can be seen that the structure of each stage is similar to the single-stage BPS estimator described in [15]. $\varphi_{i_j,j}$ denotes the i_jth test phase angle in the jth stage for $j \in \{1, 2\}$. I_j represents the number of test phase angles in the jth stage. $M(\varphi_{i_j,j}, k)$ stands for the computed distance metric corresponding to phase angle $\varphi_{i_j,j}$ for the kth symbol. $\varphi_{\hat{i}_j,j}$ denotes the phase estimate selected from the I_j test phase angles in the jth stage. N_j denotes the summing window length of the jth stage, which was forced to be identical in [18] and [19]. In the first stage, the test phase angles $\varphi_{i_1,1}$ is directly given by

$$\varphi_{i_1,1} = \frac{i_1\pi}{2I_1} - \frac{\pi}{4}, \quad i = 0, 1, \ldots, I_1 - 1 \tag{5}$$

The test phase angles $\varphi_{i_2,2}$ of the second stage is computed based on the coarse phase estimate $\varphi_{\hat{i}_1,1}$ according to

$$\varphi_{i_2,2} = \left[\varphi_{\hat{i}_1,1} - \text{ceil}\left(\frac{I_2}{2}\right)\frac{\pi}{2I_1I_2} + \frac{i_2\pi}{2I_1I_2}\right] \bmod \frac{\pi}{2}, \quad i_2 = 0, 1, \ldots, I_2. \tag{6}$$

It is worthy to note from (6) that the second stage actually contains $I_2 + 1$ test phase angles including the estimated phase angle $\varphi_{\hat{i}_1,1}$ of the first stage. However, the most of the operations for computing the distance metric of $\varphi_{\hat{i}_1,1}$ has been accomplished in the first stage, such as the phase rotation, hard decision, and squared Euclidean distance calculation. The only difference is the summing operation over different-length summing windows, which merely leads to a change of the number of real adders. Moreover, N_1 is preferred to be larger than N_2, which will be explained and demonstrated later. In this regard, there are no additional computational efforts for computing the distance metric of $\varphi_{\hat{i}_1,1}$ in the second stage. Therefore, the effective number of phase angles associated with the complexity is only I_2 for the second stage. With the parameters I_1 and I_2, the following conclusions can be readily drawn. The test-phase resolution is defined by the product of I_1 and I_2, and the entire complexity of an estimator is determined by the sum of I_1 and I_2.

In the following, vectors $\vec{\mathbf{I}} = [I_1, I_2]$ and $\vec{\mathbf{N}} = [N_1, N_2]$ are used to describe the crucial characteristics of a two-stage BPS estimator for convenience. Similarly, I and N denote the characteristics of a single-stage BPS estimator. In general, I_1, I_2, N_1, and N_2 can be arbitrary positive integers. However, several design guidelines exist to choose these parameters considering the complexity, test-phase resolution, phase noise tolerance, and pattern effect.

B. Guidelines for Complexity Minimization

Solely considering the computational effort or complexity, a straightforward guideline is to minimize $I_1 + I_2$ while keeping I_1I_2 close to I, where I denotes the minimum acceptable number of test phase angles for a single-stage BPS estimator [15]. The condition $I_1I_2 \sim I$ indicates a similar test-phase resolution of the two-stage estimator to a single-stage one. The objective of minimizing $I_1 + I_2$ means to reduce the total number of test-phase angles, thereby cutting down the entire complexity as much as possible.

$$\text{Guideline 1}: \min \quad I_1 + I_2 \quad \text{s.t.} \quad I_1I_2 \sim I$$

Taking square 64QAM as an example, the required number of test phase angles is inferred to be 64 for a single-stage estimator (i.e., $I = 64$) [15]. According to Guideline 1, the desired I_1 and I_2 are both equal to 8 (i.e., $\vec{\mathbf{I}} = [8, 8]$). Hence, the total number of test phase angles is only 16 indicating a complexity reduction by a factor of 4.

In light of Guideline 1, the number of test-phase angles in the first stage is suggested to be reduced to a small value (e.g., 8 for 64QAM). As explained in Section II.B, the pattern effect may lead to significant estimation errors in the first stage. Owing to the pattern effect, it is of high probability to make an inaccurate

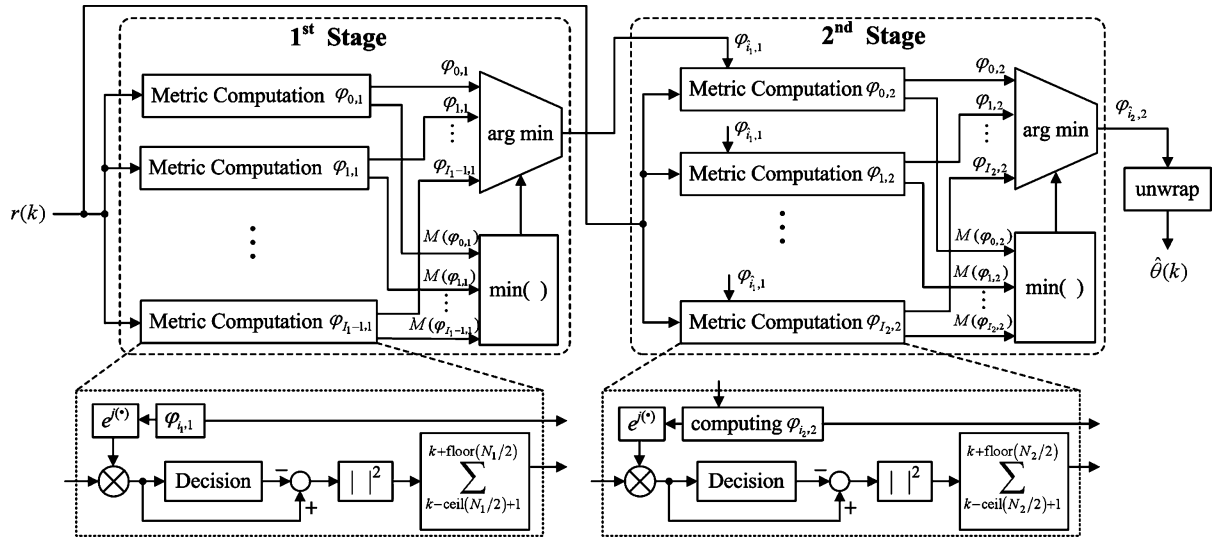

Fig. 3. Block diagram of the derived general two-stage BPS estimator.

coarse estimation in the first stage, which causes a meaningless fine phase search in the second stage. It is more convenient to understand this with the assistance of Fig. 2(b). If the number of test-phase angles are limited in the first stage (e.g., $I_1 = 8$), the coarse phase estimate may be far from the actual phase. In this case, the target minimum will be out of the searching range of the second stage according to (6). The ultimate estimation accuracy inevitably degrades. In order to mitigate the pattern effect, the key is to increase the summing window length as much as possible. Fortunately, the minimum phase search spacing becomes larger as the number of test phase angles decreases. Moreover, the minimum phase search spacing of the first stage is certainly larger than the second stage. Larger search spacing implies lower resolution and thereby allows for more significant fluctuations of phase noise in an observed summing window. Equivalently speaking, if the amount of phase noise is fixed, a longer summing window is acceptable. In this regard, it is a feasible way to appropriately extend the summing window in the first stage for mitigating the pattern effect. It is interesting that this treatment will not burden the estimator too much in terms of complexity since it merely requires several additional real adders regarding the hardware implementation.

Under the precondition of an accurate coarse estimation, the final tolerance to laser phase noise rests with the second stage. From an empirical point of view, the optimal summing window length of the second stage should approximate to that of a single-stage estimator for the sake of obtaining comparable tolerance to laser phase noise. This prediction will be verified by the simulation results in the next section. Therefore, another guideline for determining $\vec{\mathbf{N}}$ is summarized as follows:

$$\text{Guideline 2}: \quad N_1 > N_2 \approx N_{\text{opt}}$$

Here N_{opt} is the optimal length of summing window for a single-stage BPS estimator given the same SNR and laser linewidth. So far, one can realize the significance of removing the restriction of $N_1 = N_2$. This manipulation enables independent optimization of N_1 and N_2 granting a specialized role to each individual stage. The first stage mitigates the pattern effect to guarantee a reliable coarse estimation, and then the second stage tries to maintain the same tolerance to laser phase noise. If N_1 is still restricted to be equal to N_2, the estimator has to make a tradeoff between relaxing the pattern effect and preserving the same laser linewidth tolerance. This compromise will lead to some performance degradation. In sum, under the condition given by Guideline 2, the first guideline can be implemented with similar laser-linewidth tolerance.

IV. Numerical Results

By numerical simulations taking square 64QAM as example, this section is dedicated to verification and evaluation of the improved two-stage BPS estimator aided by the proposed guidelines. In our simulations, a total of 10^6 symbols were used to obtain the bit error ratio (BER) or Q-factor in dB. Every six bits were mapped into one symbol. Two of every six bits were assigned to perform differential coding for overcoming $\pi/2$ phase ambiguity [15]. The input sample sequence to an estimator is generated according to (1), where the phase noise is modeled as a Wiener process [15], and the additive complex Gaussian noise is loaded to determine E_s/N_0.

At first, a two-dimensional optimization of the two parameters N_1 and N_2 was carried out for the derived two-stage BPS estimator with $\vec{\mathbf{I}} = [8, 8]$. The product of Δf and T_s was set to a typical value of 5×10^{-5}, where Δf denotes the combined linewidth of the transmitter and receiver lasers [12], and T_s represents the symbol duration. The contour diagram is shown in Fig. 4 at $E_s/N_0 = 23$ dB. In terms of Q-factor in dB, there is one maximum located at $\vec{\mathbf{N}} = [40, 15]$ confirming $N_1 > N_2$ in the optimal case. Moreover, it is necessary to emphasize here that the optimized length of summing window of a single-stage estimator is roughly 15 as well (i.e., $N_{\text{opt}} \approx 15$) for $\Delta f \cdot T_s = 5 \times 10^{-5}$ and $E_s/N_0 = 23$ dB. The same situations happened for other values of $\Delta f \cdot T_s$ and E_s/N_0. Therefore, it is clear that the simulation results show excellent agreement with the prediction behind Guideline 2.

In order to evaluate the joint impact of pattern effect and laser linewidth in the first stage, the variance of the estimation error

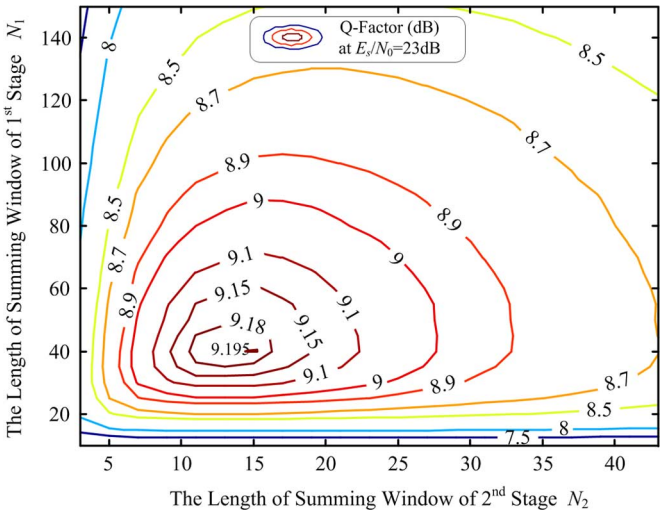

Fig. 4. Contour diagram for optimization of the parameters N_1 and N_2.

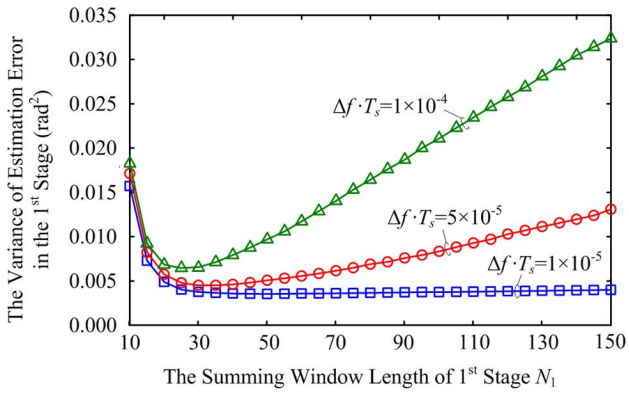

Fig. 5. Variance of estimation error versus the length of summing window in the first stage for $I_1 = 8$.

was assessed as a function of the summing window length in the first stage for $I_1 = 8$ (Fig. 5). It can be seen that there is one minimum of the estimation error corresponding to an optimal N_1 for each $\Delta f \cdot T_s$. Although N_1 is suggested to be suitably increased in order to mitigate the pattern effect, the optimal value of N_1 is still upper-bounded due to the laser linewidth. Hence, this minimum is the outcome after compromising the pattern effect and laser phase noise. It can also be observed that the optimal N_1 decreases with the increase of $\Delta f \cdot T_s$. Assuming N_2 takes the optimal value and $E_s/N_0 = 23$ dB, the Q-factor as a function of N_1 was calculated for the proposed two-stage BPS estimator with $\vec{\mathbf{I}} = [8, 8]$ at different $\Delta f \cdot T_s$ (Fig. 6). Figs. 5 and 6 show good agreement in terms of the optimal N_1. This indicates that the coarse estimation accuracy in the first stage principally influences the ultimate phase estimation accuracy and the BER.

Then, the Q-factor was investigated as a function of N_2, assuming that N_1 takes the optimal value in each case and $E_s/N_0 = 23$ dB. Fig. 7 shows the results for the proposed two-stage BPS estimator with $\vec{\mathbf{I}} = [8, 8]$ at different $\Delta f \cdot T_s$. The Q-factor as a function of N for a single-stage BPS estimator with $I = 64$ are also plotted using the blue curves for comparison. The optimized two-stage estimator shows an identical performance to a single-stage one. It means that the impact

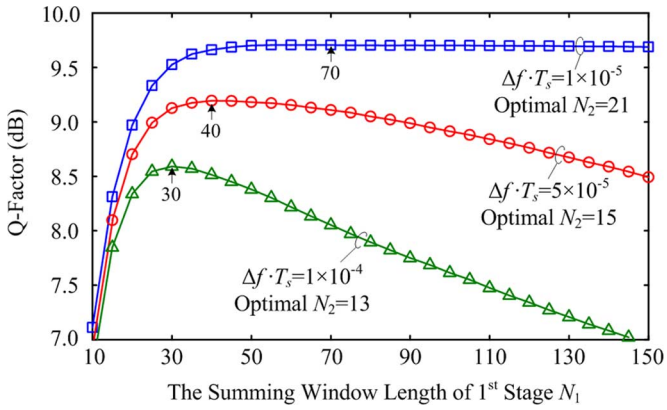

Fig. 6. Q-factor versus N_1 for the proposed two-stage BPS estimator.

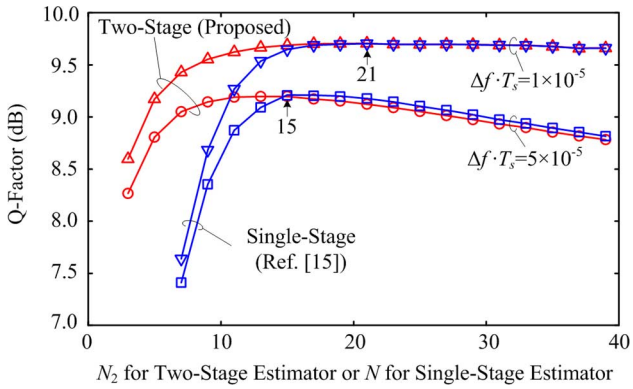

Fig. 7. Q-factor versus N_2 for the proposed two-stage BPS estimator and Q-factor versus N for the single-stage BPS estimator in [15].

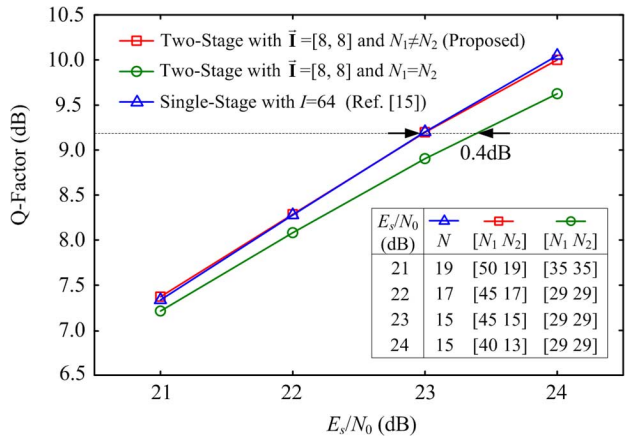

E_s/N_0 (dB)	N	$[N_1\ N_2]$	$[N_1\ N_2]$
21	19	[50 19]	[35 35]
22	17	[45 17]	[29 29]
23	15	[45 15]	[29 29]
24	15	[40 13]	[29 29]

Fig. 8. Q-factor versus E_s/N_0 for different estimators.

of the pattern effect has been mitigated to a negligible level, and meanwhile the estimation accuracy is maintained. Another important observation is that the optimal N_2 is approximately equal to the optimal N for each $\Delta f \cdot T_s$, which further verifies the prediction behind Guideline 2.

Fig. 8 compares the simulated Q-factor as a function of E_s/N_0 at $\Delta f \cdot T_s = 5 \times 10^{-5}$ for three estimators: the proposed two-stage estimator with $\vec{\mathbf{I}} = [8, 8]$, a two-stage estimator with the same $\vec{\mathbf{I}}$ but with the restriction of equal summing window length (i.e., $N_1 = N_2$), and the single stage estimator

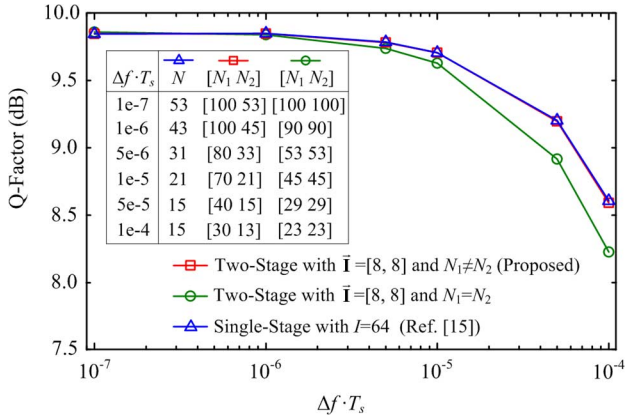

Fig. 9. Laser phase noise tolerance for different estimators.

with $I = 64$. In each case, the summing window length is optimized. The optimal summing window lengths are listed in the inset table. It can be seen that the proposed two-stage estimator with independently-optimized N_1 and N_2 exhibits almost the same performance as the single-stage estimator. In contrast, with the restriction of $N_1 = N_2$, the two-stage estimator suffers from roughly 0.4-dB sensitivity penalty at $\mathrm{BER} = 2 \times 10^{-3}$ or equivalent $\mathrm{Q-factor} = 9.18$ dB.

Fig. 9 shows the tolerance to laser phase noise at $E_s/N_0 = 23$ dB for these three estimators. In each case, the summing length window is optimized. The optimal summing window lengths are listed in the inset table.If the restriction of $N_1 = N_2$ is reserved, the two-stage estimator is subject to a larger Q-penalty. In contrast, the proposed two-stage estimator with independently- optimized N_1 and N_2 possesses comparable laser phase noise tolerance to the single-stage one.

V. Further Discussion

Although only the results of 64QAM are presented in this paper, other QAM formats with levels up to 128 were also investigated with similar results obtained. The proposed guidelines function well. However, if the QAM level further increases to 256 or even higher, some degree of performance degradation would occur in the presence of large laser linewidth due to the short summing window and significant resultant pattern effect in the first stage. In these cases, the complexity is minimized at a cost of performance, which is not advisable. Therefore, the performance is required to be taken into account in the minimization of $I_1 + I_2$ for QAM formats with 256-level and higher. Fortunately, Guideline 1 offers the possibility to elaborately change the sum of I_1 and I_2 around its minimum point, since the product of I_1 and I_2 is only forced to be close to the value of I, rather than equal to I. For example, $I = 64$ for 256 QAM. Several combinations can be obtained around the minimum point of $I_1 + I_2$, such as $\vec{\mathbf{I}} = [8\,8], [9\,7], [10\,6], [11\,6], [12\,5], \ldots$. As explained earlier, the pattern effect is mainly dependent on the value of I_1, and the pattern effect attenuates with the increase of I_1. Hence, an estimator with $\vec{\mathbf{I}} = [12\ 5]$ is a good choice in terms of performance despite of the aggravated hardware burden induced by one additional test-phase angle. In this case, the computational complexity is not globally minimal but the performance holds.

The last issue is about the stage number. Inspired by the derived two-stage configuration and proposed guidelines, one can indeed extend an estimator to have more stages. For example, a three-stage estimator is expected to have $\vec{\mathbf{I}} = [4,\ 4,\ 4]$ demonstrating a potential $\sim 5\times$ complexity reduction for 64QAM. However, in this case, the pattern effect is so severe that an extremely long summing window is commonly required in the first stage especially for higher-order formats. This will increase the computational efforts and be prohibitive in the presence of large laser phase noise and strong fiber nonlinearity. In practice, a two-stage configuration seems to be the best option in terms of complexity and performance.

VI. Conclusion

Based on the BPS algorithm, a general two-stage feed- forward carrier phase estimator has been derived by removing several restrictions assumed in the prior art. The derived two-stage estimator possesses several degrees of freedom to independently determine its crucial parameters, such as the summing window length and test-phase angle number in each individual stage. Under the framework of the generalized two-stage estimator, two major guidelines are presented to minimize the computational complexity while avoiding significant pattern effect and maintaining the tolerance to laser linewidth. As compared to the conventional single-stage BPS estimator demonstrated in [15], the derived two-stage estimator adhering to the proposed guidelines is capable of achieving 4 $\times$ reduction of computational complexity for the representative square 64QAM format.

References

[1] A. H. Gnauck, R. W. Tkach, A. R. Chraplyvy, and T. Li, "High-capacity optical transmission systems," *J. Lightw. Technol.*, vol. 26, no. 9, pp. 1032–1045, May 2008.

[2] P. J. Winzer, A. H. Gnauck, C. R. Doerr, M. Magarini, and L. L. Buhl, "Spectrally efficient long-haul optical networking using 112-Gb/s polarization-multiplexed 16-QAM," *J. Lightw. Technol.*, vol. 28, no. 4, pp. 547–556, Feb. 2010.

[3] X. Zhou and J. Yu, "Multi-level, multi-dimensional coding for high-speed and high spectral-efficiency optical transmission," *J. Lightw. Technol.*, vol. 27, no. 16, pp. 3641–3653, Aug. 2010.

[4] X. Zhou and J. Yu, "200-Gb/s PDM-16QAM generation using a new synthesizing method," in *Proc. ECOC*, Vienna, Austria, 2009, Paper10.3.5.

[5] J. Yu, X. Zhou, Y. K. Huang, S. Gupta, M. F. Huang, T. Wang, and P. Magill, "112.8-Gb/s PM-RZ-64QAM optical signal generation and transmission on a 12.5 GHz WDM grid," in *Proc. OFC*, Mar. 2010, PaperOThM1.

[6] E. M. Ip and J. M. Kahn, "Fiber impairment compensation using coherent detection and digital signal processing," *J. Lightw. Technol.*, vol. 28, no. 4, pp. 502–519, Feb. 2010.

[7] G. Li, "Recent advances in coherent optical communication," *Adv. Opt. Photon.*, vol. 1, pp. 279–307, 2009.

[8] E. Ip and J. Kahn, "Feedforward carrier recovery for coherent optical communication," *J. Lightw. Technol.*, vol. 25, no. 9, pp. 2675–2692, Sep. 2007.

[9] R. Noé, "Phase noise tolerant synchronous QPSK/BPSK baseband-type intradyne receiver concept with feed-forward carrier recovery," *J. Lightw. Technol.*, vol. 23, no. 2, pp. 802–808, Feb. 2005.

[10] H. Louchet, K. Kuzmin, and A. Richter, "Improved DSP algorithms for coherent 16-QAM transmission," in *Proc. ECOC*, Brussels, Belgium, Sep. 21–25, 2008, PaperTu.1.E.6.

[11] M. Seimetz, "Laser linewidth limitations for optical systems with high-order modulation employing feedforward digital carrier phase estimation," in *Proc. OFC*, San Diego, CA, Feb. 24–28, 2008, PaperOTuM2.

[12] I. Fatadin, D. Ives, and S. J. Savory, "Laser linewidth tolerance for 16QAM coherent optical systems using QPSK partitioning," *IEEE Photon. Technol. Lett.*, vol. 22, no. 9, pp. 631–633, May 2010.
[13] S. K. Oh and S. P. Stapleion, "Blind phase recovery using finite alphabet properties in digital communications," *Electron. Lett.*, vol. 33, no. 3, pp. 175–176, Jan. 1997.
[14] F. Rice, B. Cowley, B. Moran, and M. Rice, "Cramér-Rao lower bounds for QAM phase and frequency estimation," *IEEE Trans. Commun.*, vol. 49, no. 9, pp. 1582–1591, Sep. 2001.
[15] T. Pfau, S. Hoffmann, and R. Noé, "Hardware-efficient coherent digital receiver concept with feedforward carrier recovery for M-QAM constellations," *J. Lightw. Technol.*, vol. 27, no. 8, pp. 989–999, Apr. 2009.
[16] T. Pfau and R. Noé, "Phase-noise-tolerant two-stage carrier recovery concept for higher order QAM formats," *IEEE J. Sel. Topics Quantum Electron.*, vol. 16, no. 5, pp. 1210–1216, Sep.–Oct. 2010.
[17] X. Zhou, "An improved feed-forward carrier recovery algorithm for coherent receivers with M-QAM modulation format," *IEEE Photon. Technol. Lett.*, vol. 22, no. 14, pp. 1051–1053, Jul. 2010.
[18] X. Li, Y. Cao, S. Yu, W. Gu, and Y. Ji, "A simplified feed-forward carrier recovery algorithm for coherent optical QAM system," *J. Lightw. Technol.*, vol. 29, no. 5, pp. 801–807, Mar. 2011.
[19] Q. Zhuge, C. Chen, and D. V. Plant, "Low computation complexity two-stage feedforward carrier recovery algorithm for M-QAM," presented at the OFC2011, Los Angeles, CA, Mar. 2011.

Jianqiang Li (S'05–M'10) received the B.E. and Ph.D. degrees (both with honors) from Beijing University of Posts and Telecommunications, Beijing, China, in 2005 and 2009, respectively.

In July 2009, he joined in Fujitsu R&D Center (FRDC), Beijing, China, where he was engaged in research on high-speed and high-capacity optical communication technologies. Since June 2011, he has been with Photonics Laboratory, Department of Microtechnology and Nanoscience, Chalmers University of Technology, Gothenburg, Sweden, as a Postdoctoral Fellow. His research interests include optical communications systems, microwave photonics and radio-over-fiber systems.

Lei Li received the B.S. degree in information and communication engineering from Xi'an Jiaotong University, Xi'an, China, in 1999, and the M.S. degree in electrical engineering from the University of Toledo, Toledo, OH, in 2002.

He joined in Fujitsu R&D Center (FRDC), Beijing, China, in 2002, and since 2006 he has been engaged in research and development in optical digital coherent technologies.

Zhenning Tao (S'98–M'01–SM'09) received the B.S. degree in physics and Ph.D. degree in communications and information systems from Peking University, Beijing, China, in 1996 and 2001, respectively.

He joined in Fujitsu R&D Center (FRDC), Beijing, China, in 2001 to work on research and development of optical fiber communication system and subsystems. His current research interests focus on optical digital coherent technologies.

Dr. Tao received the Institute of Electronics, Information and Communication Engineers (IEICE) Optical Communication Systems (OCS) Best Paper Award in 2008 and Fujitsu Laboratory President Award in 2010.

Takeshi Hoshida (S'97–M'98) received the B.E., M.E., and Ph.D. degrees in electronic engineering from the University of Tokyo, Tokyo, Japan, in 1993, 1995, and 1998, respectively.

From 1998 to 2000, he was with Fujitsu Laboratories Ltd., Kawasaki, Japan. From 2000 to 2002, he was with Fujitsu Network Communications, Inc., Richardson, TX. Since 2002, he has been with Fujitsu Laboratories Ltd., Kawasaki, Japan, where he has been engaged in the research and development of DWDM optical transmission systems. Since 2007, he has also been with Fujitsu Limited, Kawasaki, Japan.

Dr. Hoshida is a member of the Institute of Electronics, Information and Communications Engineers (IEICE) and the Japan Society of Applied Physics.

Jens C. Rasmussen (S'95–M'99) received the Dipl.-Ing. and Dr.-Ing. degrees from the RWTH Aachen University, Aachen, Germany, in 1993 and 1998, respectively.

In 2000, he joined Fujitsu Laboratories Ltd., Kawasaki, Japan, and has been engaged since then in research and development of DWDM optical transmission systems. Since 2007, he has also been with Fujitsu Limited, Kawasaki, Japan.

Dr. Rasmussen was awarded a scholarship entitled "Two years language and training in Japan," in 1998 by the German Academic Exchange Service DAAD.